2018 Annual American Control Conference (ACC)
June 27–29, 2018. Wisconsin Center, Milwaukee, USA

Optimization of Output Functions with Nonholonomic Virtual Constraints in Underactuated Bipedal Walking Control

Wai Kei Chan[1], Yan Gu[2] and Bin Yao[1]

Abstract— **Underactuation is a challenging issue to deal with in bipedal walking control. Because of the highly nonlinear behaviors of bipedal robotic walking, nonlinear control theories, especially state feedback control based on input-output feedback linearization, has been applied to achieve stable walking. For underactuated bipeds, control design based on input-output linearization can result in internal dynamics whose stability and convergence rate to the desired gait affect the closed-loop stability and the overall convergence rate. Because the stability and the convergence rate of the internal dynamics can only be affected by the output function design, this paper proposes a general output function design to allow for greater freedom in output function optimization and better control performance as compared with previous studies. The proposed output function design and optimization, as well as the input-output linearizing controller, are simulated on a planar bipedal robot to validate the fast convergence rate to desired gait and the high robustness to external disturbances of the proposed method.**

I. INTRODUCTION

Bipedal walking control has been extensively studied for decades. Besides the well-known concepts such as Zero Moment Point (ZMP) [1] [2] and Capture Point [3], which evaluate walking stability based on some ground-reference points, stable walking has also been achieved through nonlinear control design such as the Hybrid Zero Dynamics (HZD) approach [4]. Some of the distinctive features of the HZD approach are that stable walking can be achieved in the presence of underactuation and that the walking stability can be guaranteed in a provable way.

In the HZD approach, foot landing is modeled as a rigid impact between the foot and the ground with an infinitesimally short impulse effect. During the landing impact, a discrete jump in the joint velocity is generated, but the joint position evolution remains continuous. With this impact modeling, the walking dynamics is established to include a continuous swing motion and a discrete landing effect. For underactuated bipeds, due to the lack of control effort at the unactuated joint, internal dynamics exist within the system that utilizes input-output feedback linearization for controller design. The internal dynamics become hybrid zero dynamics when the output functions are identically zero throughout the entire walking process that includes continuous and discrete phases. In the controller design, the output functions are defined as the tracking errors between the actual trajectories and the desired walking gait. Therefore, trajectory tracking control can be carried out by using state feedback control with input-output linearization that drives the output functions to zero exponentially fast. The walking stability is then ensured based on the Poincaré method. In this HZD framework, HZD can be constructed with a proper design of the desired walking pattern for bipedal robotic walking with one degree of underactuation [5]. With the concept of HZD for underactuated bipeds, the walking stability can be evaluated through the resulting HZD that implies the stability of the overall system. As a result, the dimensions of stability analysis for the biped system is greatly reduced. In addition to underactuated walking, the HZD framework has enabled orbital stabilization of fully-actuated bipedal walking [6]. Moreover, angular momentum has been used for output function design in order to achieve better control performance, such as better robustness regarding the external disturbances, as compared with the configuration-based output function design [7]. In contrast to the ground-reference points based approaches, the HZD approach can achieve high-speed periodic walking with high performance including formally provable stability, agility, and energy efficiency.

Previously, time-dependent orbital stabilization of underactuated bipedal walking has been achieved by synthesizing a time-dependent walking gait into the output function design [9]. Instead of using Poincaré map, this work evaluates the walking stability through the monodromy matrix of the variational equations of the equivalent transformed autonomous system. Given that the internal dynamics can only be affected by the output function definitions when input-output linearization is utilized for control design, an output function optimization method, which exploits the effect of modifying the output function definition on the resulting internal dynamics, is then proposed to improve the control performance [10]. By optimizing the linear combination of the position tracking errors in the output function definition to satisfy the stability criterion, walking stabilization for underactuated bipeds has also been achieved with this approach. However, the output functions have only been defined as the position tracking errors, which limits the design freedom in the optimization process. In this study, a general output function design is proposed, which includes both position and velocity tracking errors. With the additional design freedom, control performance, such as convergence rate to the desired trajectories and the robustness to external disturbances, can be improved by further optimizing the output functions from the previous work in [10].

[1]Wai Kei Chan and Bin Yao are with the School of Mechanical Engineering, Purdue University, West Lafayette, IN 47907, U.S.A. Email: chan165@purdue.edu, byao@purdue.edu

[2]Yan Gu is with the school of Mechanical Engineering, University of Massachusetts Lowell, Lowell, MA 01854, U.S.A. Email: Yan_Gu@uml.edu

The rest of the paper will be presented in the following structure. Section II introduces the full-order hybrid walking model, the proposed output function design, and the state feedback controller design. The stability criterion based on monodromy matrices and the output function optimization are explained in Section III. Section IV presents the simulation results.

II. BIPEDAL WALKING CONTROL

The goal of the control design in this study is to achieve orbitally exponential stabilization of underactuated walking based on nonlinear control theories. In this section, the dynamic model of bipedal robotic walking is presented. According to the HZD approach, a complete step includes a continuous swing motion and a discrete landing impact with an impulse effect [4]. To perform trajectory tracking control, the proposed output function design and the state feedback controller design based on input-output feedback linearization are utilized to drive all of the output functions to zero exponentially fast during continuous phases. As a result, all of the actuated joints will converge to their desired trajectories during continuous phases. However, due to underactuation, internal dynamics exist within the system, and the entire closed-loop system may still be unstable. Therefore, a systematic optimization method is introduced in Section III, which, along with the proposed controller design in this section, guarantees the closed-loop stability.

A. Hybrid Bipedal Walking Dynamics

In bipedal walking, a full step typically includes two phases, a Single Support Phase (SSP) and a Double Support Phase (DSP). In an SSP, there is a support foot, which is in contact with the ground, and a swing foot, which swings in the air. Same as the HZD framework, the following assumptions are made to simplify the complicated walking behaviors [4]:

1) The DSP is assumed to be infinitesimally short;
2) At a landing, there is no rebound or slipping between the swing foot and the ground, and the support foot immediately leaves the ground without further interaction with the ground until the next landing.

According to the assumptions above, the contact point between the support foot and the ground serves as a pin joint of the biped during an SSP. The dynamics of the swing motion can be obtained by using the Lagrange's equation [11]. At the instantaneous DSP, the rigid impact happens in an infinitesimal period of time. Similar to the previous work [4] [9], the impact can be modeled as an impulse effect, which results in a discrete jump in joint velocities. These jumps can also be described as a function that represents the differences between the states right before an impact and right after an impact.

The biped model considered in this study is a planar robot with five revolute joints, two identical point feet, and a torso. As shown in Fig. 1, the biped has four actuators, and thus one degree of underactuation exists. The full-order walking

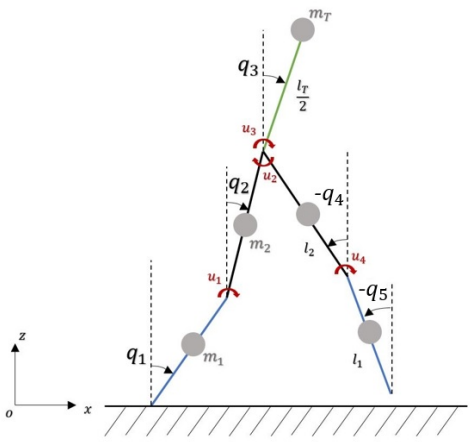

Fig. 1. A planar bipedal robot with five revolute joints. The masses are lumped at the link centers. l_1 and l_2 are the lengths of the lower and the upper limbs, respectively, and l_r is the torso length.

dynamics of the bipedal robot can be obtained as:

$$\begin{cases} \mathbf{M}(\mathbf{q})\ddot{\mathbf{q}} + \mathbf{h}(\mathbf{q},\dot{\mathbf{q}}) = \mathbf{B}_u\mathbf{u}, & \text{if} \quad \mathbf{q} \notin S_q(\mathbf{q},\dot{\mathbf{q}}); \\ [\mathbf{q}(t^+)^T, \dot{\mathbf{q}}(t^+)^T]^T = \mathbf{I}_q(\mathbf{q},\dot{\mathbf{q}}), & \text{if} \quad \mathbf{q} \in S_q(\mathbf{q},\dot{\mathbf{q}}); \end{cases} \tag{1}$$

where $\mathbf{q}, \dot{\mathbf{q}}, \ddot{\mathbf{q}} \in \mathbb{R}^5$ are the joint positions, velocities, and accelerations, respectively, $\mathbf{M}(\mathbf{q}) \in \mathbb{R}^{5\text{x}5}$ is the inertia matrix, $\mathbf{h}(\mathbf{q},\dot{\mathbf{q}}) \in \mathbb{R}^5$ is the sum of Coriolis, centrifugal and gravitational terms, $\mathbf{B}_u \in \mathbb{R}^{5\text{x}4}$ is the input matrix, $\mathbf{u} \in \mathbb{R}^4$ is the joint-torque input, and $\mathbf{I}_q$ represents the DSP reset map that initializes the state variables for the next step by mapping them from the states right before an impact, $(\mathbf{q}(t^-), \dot{\mathbf{q}}(t^-))$, to the states right after an impact, $(\mathbf{q}(t^+), \dot{\mathbf{q}}(t^+))$. The switching surface $S_q(\mathbf{q},\dot{\mathbf{q}})$ is defined as

$$S_q(\mathbf{q},\dot{\mathbf{q}}) := \{\mathbf{q},\dot{\mathbf{q}} \in \mathbb{R}^5 : \mathrm{h_{sw}}(\mathbf{q}) = 0, \frac{\partial \mathrm{h_{sw}}}{\partial \mathbf{q}}\dot{\mathbf{q}} < 0\}, \tag{2}$$

where $h_{sw}(\mathbf{q})$ is the swing foot height.

Define

$$\mathbf{x} := \begin{bmatrix} \mathbf{x}_1 \\ \mathbf{x}_2 \end{bmatrix} \in \mathbb{R}^{10}, \tag{4}$$

where $\mathbf{x}_1 := \mathbf{q} \in \mathbb{R}^5$ and $\mathbf{x}_2 := \dot{\mathbf{q}} \in \mathbb{R}^5$. The whole system can be expressed in the state-space form as:

$$\begin{cases} \dot{\mathbf{x}} = \begin{bmatrix} \mathbf{x}_2 \\ \mathbf{f}(x) + \mathbf{g}(x)\mathbf{u} \end{bmatrix}, & \text{if} \quad \mathbf{x} \notin S(\mathbf{x}); \\ \Delta\mathbf{x} = \mathbf{I}(\mathbf{x}), & \text{if} \quad \mathbf{x} \in S(\mathbf{x}); \end{cases} \tag{3}$$

where $\mathbf{f}(\mathbf{x}) := -\mathbf{M}^{-1}\mathbf{h}$, $\mathbf{g}(\mathbf{x}) := \mathbf{M}^{-1}\mathbf{B}_u$, $\Delta\mathbf{x} := \mathbf{x}(t^+) - \mathbf{x}(t^-)$, $\mathbf{I}(\mathbf{x})$ represents the reset map, and $S(\mathbf{x})$ represents the switching surface. $\mathbf{I}(\mathbf{x})$ can be obtained based on $\mathbf{I}_q(\mathbf{q},\dot{\mathbf{q}})$. The switching surface now becomes

$$S(\mathbf{x}) := \{\mathbf{x} \in \mathbb{R}^{10} : \psi(\mathbf{x}) := \mathrm{h_{sw}}(\mathbf{x}_1) = 0, \frac{\partial \psi(\mathbf{x})}{\partial \mathbf{x}_1}\mathbf{x}_2 < 0\}. \tag{4}$$

B. Output Function Design

In order to stabilize underactuated walking, state feedback control based on input-output feedback linearization is utilized for trajectory tracking control. Because the output function definition involves the desired walking trajectories $\bar{\mathbf{q}}_d(t)$, it is necessary to plan $\bar{\mathbf{q}}_d(t)$ in the first place. Previously, optimization methods based on Bézier curve parameterization have been utilized to find the desired gait with minimized torque consumption and desirable walking speed and step distance [10] [12]. To obtain a practical gait $\mathbf{q}_d(t)$ associated with the actual landing moments, adjustments have been made to this previous optimization methods [9].

Let

$$\mathbf{q} = [q_1, q_2, q_3, q_4, q_5]^T \in \mathbb{R}^5$$

and

$$\mathbf{u} = [u_1, u_2, u_3, u_4]^T \in \mathbb{R}^4$$

be the joint positions and the torque inputs, respectively. Previously, the output functions are defined as the linear combination of the position tracking errors [10], i.e.,

$$\mathbf{y}(t) = \mathbf{H}(\mathbf{H}_T(\mathbf{q}(t) - \mathbf{q}_d(t)), \tag{5}$$

where

$$\mathbf{H} := \begin{bmatrix} 0 & 1 & 0 & 0 & 0 \\ 0 & 0 & 1 & 0 & 0 \\ 0 & 0 & 0 & 1 & 0 \\ 0 & 0 & 0 & 0 & 1 \end{bmatrix}$$

and $\mathbf{H}_T \in \mathbb{R}^{5\text{x}5}$ is a nonsingular matrix. The resulting internal dynamics can be stabilized by optimizing the constant matrix $\mathbf{H}_T \in \mathbb{R}^{5\text{x}5}$ in the output functions. This study takes a further step based on this previous output function design by including the velocity terms so as to obtain a more general class of output functions with additional design freedom. The proposed output functions can be expressed as

$$\mathbf{y}(t) = \mathbf{H}(\mathbf{H}_{Tp}(\mathbf{q}(t) - \mathbf{q}_d(t)) + \mathbf{H}_{Tv}(\dot{\mathbf{q}}(t) - \dot{\mathbf{q}}_d(t))), \tag{6}$$

where $\mathbf{H}_{Tp} \in \mathbb{R}^{5\text{x}5}$ and $\mathbf{H}_{Tv} \in \mathbb{R}^{5\text{x}5}$ are two independent constant matrices representing the linear combinations of the tracking errors.

To show the improvements of the proposed output function design as compared with previous work, the simulation results will be discussed for the following two cases:

Case 1 : $\mathbf{H}_{Tp}$ *is nonsingular and* $\mathbf{H}_{Tv}$ *is a zero matrix.*
With the zero matrix $\mathbf{H}_{Tv}$, the nonholonomic terms in the ouput function can be eliminated, and the output functions are equivalent to the one in Equation (5) as in prior work [9].

Case 2 : *Both of the matrices* $\mathbf{H}_{Tp}$ *and* $\mathbf{H}_{Tv}$ *are nonsingular.*
Given the nonsingular $\mathbf{H}_{Tv}$, the output function now has a general form that includes both of position and velocity tracking errors.

C. State Feedback Controller Design

Given the output function design in Equation (6), the state feedback controller design will be synthesized based on input-output linearization [13]. Due to the space limit, the controller design for ***Case 1*** is omitted. The controller design for ***Case 2*** is presented next.

Assume that there are no modeling errors or disturbances. For convenience, define a transformed state $\mathbf{x}_T$ as

$$\mathbf{x}_T := \begin{bmatrix} \mathbf{x}_{T1} \\ \mathbf{x}_{T2} \end{bmatrix} = \begin{bmatrix} \mathbf{q}_T \\ \dot{\mathbf{q}}_T \end{bmatrix} = \begin{bmatrix} \mathbf{H}_{Tv}\mathbf{q} \\ \mathbf{H}_{Tv}\dot{\mathbf{q}} \end{bmatrix} \in \mathbb{R}^{10}, \tag{7}$$

where $\mathbf{q}_T := [q_{T1}, q_{T2}, q_{T3}, q_{T4}, q_{T5}]^T$. Accordingly, the desired gait can be transformed to

$$\mathbf{q}_{Td} := [q_{T1d}, q_{T2d}, q_{T3d}, q_{T4d}, q_{T5d}]^T = \mathbf{H}_{Tv}\mathbf{q}_d. \tag{8}$$

Then, the dynamics of the SSP can be rewritten as

$$\dot{\mathbf{x}}_T := \begin{bmatrix} \dot{\mathbf{x}}_{T1} \\ \dot{\mathbf{x}}_{T2} \end{bmatrix} = \begin{bmatrix} \mathbf{x}_{T2} \\ \mathbf{f}_T + \mathbf{g}_T\mathbf{u} \end{bmatrix}, \tag{9}$$

where $\mathbf{f}_T := -\mathbf{M}_T^{-1}\mathbf{h}$, $\mathbf{g}_T := \mathbf{M}_T^{-1}\mathbf{B}_u$, $\mathbf{M}_T := \mathbf{M}(\mathbf{H}_{Tv}^{-1}\mathbf{x}_{T1})\mathbf{H}_{Tv}^{-1}$, and $\mathbf{h}_T(\mathbf{x}_T) := \mathbf{h}(\mathbf{H}_{Tv}^{-1}\mathbf{x}_{T1}, \mathbf{H}_{Tv}^{-1}\mathbf{x}_{T2})$. The output functions can now be written as

$$\mathbf{y}(t) = \mathbf{H}(\mathbf{H}_{Tp}\mathbf{H}_{Tv}^{-1}(\mathbf{x}_{T1} - \mathbf{q}_{Td}(t)) + (\mathbf{x}_{T2} - \dot{\mathbf{q}}_{Td}(t))). \tag{10}$$

Taking the first derivative on both sides of the Equation (10) and substituting the dynamics (9) into it, one obtains the following output dynamics:

$$\dot{\mathbf{y}}(t) = \mathbf{H}(\mathbf{H}_{Tp}\mathbf{H}_{Tv}^{-1}(\mathbf{x}_{T2} - \dot{\mathbf{q}}_{Td}(t)) + (\mathbf{f}_T + \mathbf{g}_T\mathbf{u} - \ddot{\mathbf{q}}_{Td}(t))). \tag{11}$$

Input-output feedback linearization is utilized here to cancel all the nonlinear terms and add a virtual controller for the linearized dynamics. Following this concept, the controller can be obtained as

$$\mathbf{u} = (\mathbf{H}\mathbf{g}_T)^{-1}(\mathbf{v} + \mathbf{H}(\ddot{\mathbf{q}}_{Td} - \mathbf{f}_T) - \mathbf{H}\mathbf{H}_{Tp}\mathbf{H}_{Tv}^{-1}(\mathbf{x}_{T2} - \dot{\mathbf{q}}_{Td}(t))), \tag{12}$$

which linearizes the nonlinear output dynamics into

$$\dot{\mathbf{y}} = \mathbf{v}. \tag{13}$$

Because of the first-order output dynamics, the virtual control law can be designed as a proportional controller. Therefore, let

$$\mathbf{v} = -\mathbf{K}_p\mathbf{y}, \tag{14}$$

where $\mathbf{K}_p \in \mathbb{R}^{4\times4}$ is a diagonal matrix. Then, the linear dynamics of the output functions can be transformed into:

$$\dot{\mathbf{y}}(t) = -\mathbf{K}_p\mathbf{y}. \tag{15}$$

As long as $\mathbf{K}_p$ is designed to be positive definite, $-\mathbf{K}_p$ is a Hurwitz matrix, and the linearized system $\dot{\mathbf{y}} = -\mathbf{K}_p\mathbf{y}$ is asymptotically stable, i.e., the output functions $\mathbf{y}$ will converge to zero exponentially fast during each SSP.

III. Stability-Based Output Function Optimization

The stability criterion based on monodromy matrix is established in [9]. Because of the time-dependent desired gait, the state-space model obtained in the last section is an aperiodic time-varying hybrid closed-loop system, whose stability is challenging to evaluate. Therefore, before applying the stability criterion to evaluate the stability of the internal dynamics, system transformation is performed to obtain an equivalent augmented autonomous system [9].

First, a phase indicator is introduced as

$$\rho = t - T_k, \qquad \forall t \in (T_k, T_{k+1}], \qquad k = 0, 1, ... \quad (16)$$

where T_k is the k^{th} actual landing moment. Then, the state-space system can be transformed into an equivalent autonomous system:

$$\begin{cases} \dot{\mathbf{x}}_{Te} = \begin{bmatrix} 1 \\ \mathbf{x}_{T2} \\ \mathbf{f}_T + \mathbf{g}_T \mathbf{u} \end{bmatrix} = \mathbf{A}_e(\mathbf{x}_{Te}), & \text{if} \quad \mathbf{x}_{Te} \notin S_{Te}(\mathbf{x}_{Te}); \\ \Delta \mathbf{x}_{Te} = \mathbf{I}_{Te}(\mathbf{x}_e), & \text{if} \quad \mathbf{x}_{Te} \in S_{Te}(\mathbf{x}_{Te}); \end{cases} \quad (17)$$

where the augmented states are defined as

$$\mathbf{x}_{Te} = \begin{bmatrix} \rho \\ \mathbf{x}_{T1} \\ \mathbf{x}_{T2} \end{bmatrix} \in \mathbb{R}^{11}, \quad (18)$$

the augmented reset function can be obtained as

$$\mathbf{I}_{Te} := \begin{bmatrix} -\rho \\ \begin{bmatrix} \mathbf{H}_{Tv} & \mathbf{0}_{5x5} \\ \mathbf{0}_{5x5} & \mathbf{H}_{Tv} \end{bmatrix} \mathbf{I}_q(\mathbf{H}_{Tv}^{-1}\mathbf{x}_{T1}, \mathbf{H}_{Tv}^{-1}\mathbf{x}_{T2}) \end{bmatrix}, \quad (19)$$

and the switching surface for the augmented system is defined as

$$S_{Te}(\mathbf{x}_{Te}) := \{\mathbf{x}_{Te} \in \mathbb{R}^{11} : \psi_e(\mathbf{x}_{Te}) := h_{sw}(\mathbf{H}_T^{-1}\mathbf{x}_{T1}) = 0, \frac{\partial \psi(\mathbf{x}_{Te})}{\partial \mathbf{x}_{Te}} \mathbf{A}_e(\mathbf{x}_{Te}) < 0\}. \quad (20)$$

A. Stability Criterion

Based on the resulting augmented autonomous system, the associated variational equations can be obtained as [14]:

$$\begin{cases} \frac{\partial \mathbf{z}_e}{\partial t} = \frac{\partial \mathbf{A}_e}{\partial \mathbf{x}_{Te}} \mathbf{A}_e(\bar{\mathbf{x}}_{Ted}(t)) \mathbf{z}_e, & \text{if} \quad t \neq \tau_k; \\ \Delta \mathbf{z}_e = \mathbf{M}_{ke} \mathbf{z}_e, & \text{if} \quad t \in \tau_k; \end{cases} \quad (21)$$

where

$$\mathbf{M}_{ke} = \frac{\partial \mathbf{I}_{Te}}{\partial \mathbf{x}_{Te}} + [\mathbf{A}_e^+ - \mathbf{A}_e - \frac{\partial \mathbf{I}_{Te}}{\partial \mathbf{x}_{Te}} \mathbf{A}_e] \frac{\frac{\partial \psi_e}{\partial \mathbf{x}_{Te}}}{\frac{\partial \psi_e}{\partial \mathbf{x}_{Te}} \mathbf{A}_e}$$

with

$$\mathbf{A}_e = \mathbf{A}_e(\bar{\mathbf{x}}_{Ted}(\tau_k)), \qquad \mathbf{A}_e^+ = \mathbf{A}_e(\bar{\mathbf{x}}_{Ted}(\tau_k^+)),$$

$$\frac{\partial \mathbf{I}_{Te}}{\partial \mathbf{x}_{Te}} = \frac{\partial \mathbf{I}_{Te}}{\partial \mathbf{x}_{Te}}(\bar{\mathbf{x}}_{Ted}(\tau_k)), \qquad \frac{\partial \psi_e}{\partial \mathbf{x}_{Te}} = \frac{\partial \psi_e}{\partial \mathbf{x}_{Te}}(\bar{\mathbf{x}}_{Ted}(\tau_k)),$$

and τ_k is the k^{th} landing moment of the desired gait.

Based on the equivalent augmented system in Equation (17), the stability criterion of the closed-loop system can be established [9]. If the solution $\bar{\mathbf{x}}_d(t)$ of the closed-loop system in Equation (3) satisfies the following conditions:

- (A1) $\frac{\partial \psi}{\partial \mathbf{x}}(\bar{\mathbf{x}}_d(\tau_k))\dot{\bar{\mathbf{x}}}_d(\tau_k) \neq 0$;
- (A2) There is no rebound and slipping between the swing foot and the ground at the impact;
- (A3) The monodromy matrix of the variational equations (21) has only one eigenvalue of unity modulus, and the moduli of all the other eigenvalues are strictly less than one.

Then, the solution $\bar{\mathbf{x}}_d(t)$ is a locally orbitally stable solution, i.e., the actual trajectories of the biped will converge to the desired orbit exponentially fast.

B. Output Function Optimization

With the stability criterion above, the stability of the closed-loop system in Equation (3) can be evaluated by checking the monodromy matrix of the variational equations of the equivalent autonomous augmented system. Recall that the stability of the entire closed-loop system can be implied by the stability of the resulting internal dynamics and that the internal dynamics can only be affected by the output function definition when input-output feedback linearization is used for control design. Therefore, the goal of the output function optimization is to search for a specific pair of $\mathbf{H}_{Tp}$ and $\mathbf{H}_{Tv}$ such that the monodromy matrix of the associated variational equations has only one eigenvalue of unity modulus and that all the other eigenvalues have moduli strictly less than one. Accordingly, the cost function is defined as the second largest modulus of all the eigenvalue, λ_s, of the monodromy matrix. Thus, the optimization problem is formulated as:

$$\text{minimize} \quad \lambda_s$$

$$\text{subject to} \quad \begin{cases} \dot{\mathbf{x}} := \begin{bmatrix} \mathbf{x}_2 \\ \mathbf{f}(x) + \mathbf{g}(x)\mathbf{u} \end{bmatrix}, & \text{if} \quad \mathbf{x} \notin S(\mathbf{x}); \\ \Delta \mathbf{x} = \mathbf{I}(\mathbf{x}), & \text{if} \quad \mathbf{x} \in S(\mathbf{x}). \end{cases}$$

Because it is challenging to optimize two 5×5 nonsingular matrices simultaneously, the optimization procedure will include two steps. First, the output functions in ***Case 1*** is utilized to find stable solutions with a specific constant matrix $\mathbf{H}_T$. Second, fix $\mathbf{H}_{Tp}$ as the optimized $\mathbf{H}_T$ in (6). The optimized constant matrix $\mathbf{H}_{Tv}$ can be found by further optimize the output function from the first step. The optimization results will be presented along with the simulations in the next section.

IV. Simulation Results

In this section, simulation results on a planar bipedal robot (see Fig.1) will be presented.

With the optimization method proposed in Section III, the control gain is chosen as

$$\mathbf{K}_p = diag(40000, 40000, 40000, 40000),$$

and the constant matrices $\mathbf{H}_{Tp}$ and $\mathbf{H}_{Tv}$ in (6) are optimized to be:

$$\mathrm{H}_{Tp} = \begin{bmatrix} -0.14 & 0.22 & 0.46 & -0.01 & -0.55 \\ -0.82 & 0.87 & 21.79 & -22.09 & 1.95 \\ 0.06 & 0.01 & -21.79 & 22 & -0.15 \\ -0.06 & 0.27 & -1.73 & 2.25 & 0.71 \\ 1.08 & -1.33 & 15.29 & -15.13 & -1.02 \end{bmatrix};$$

$$H_{Tv} = \begin{bmatrix} 0.84 & 5.12 & 1.11 & -0.32 & 2.90 \\ -0.44 & 1.67 & 6.83 & -0.45 & 3.18 \\ 0.75 & 1.08 & 1.46 & 3.18 & 3.19 \\ -0.97 & 0.65 & 0.51 & 1.1 & 4.93 \\ 0.1 & -0.06 & 0.58 & -0.68 & 1.55 \end{bmatrix}.$$

Then, the eigenvalues of the monodromy matrices corresponding to *Case 1* and *Case 2* are computed as:
Case 1 : $1.00, 0.95, 0.72, 0, 0, 0, 0, 0, 0, 0$;
Case 2 : $1.00, 0.57, 0.5, 0.5, 0.48, 0.48, 0.0012, 0, 0, 0, 0$.

A. Orbitally Exponential Stabilization

The validity of the proposed control design is shown in a fifteen-step walking simulation (see Fig. 2). Physical parameters of the biped model are given in Table. 1.

TABLE I
PHYSICAL PARAMETERS OF THE SIMULATED BIPEDAL MODEL

$m_1(kg)$	$m_2(kg)$	$m_T(kg)$	$l_1, l_2, \frac{r}{2}(m)$
3	6	10	0.4

To show the validity of the proposed control design, the biped model is simulated with some initial tracking errors. Simulation results in Fig. 2 show that the biped is able to recover from the initial tracking errors, i.e., stable walking is achieved under the proposed state feedback control law and the output function optimization. However, the actual trajectories do not converge to the desired trajectories $\bar{\mathbf{q}}_d$ but the desired orbit instead. As shown in the figure, there exists a constant time shift between the actual trajectories and the desired gait $\bar{\mathbf{q}}_d$, which indicates that the simulated walking is orbitally stable.

B. Convergence Rate to the Desired Gait

Orbital stability of a bipedal walking system can be evaluated in multiple ways. In this study, the stability criterion based on variational equations is utilized to evaluate the stability of the entire closed-loop system. By minimizing the eigenvalues of the monodromy matrix, the stability of the resulting internal dynamics, which determines the closed-loop stability, can be guaranteed. In addition, the eigenvalues of the monodromy matrix of a system can determine the closed-loop convergence rate. In the output function optimization, the cost function is defined as the second largest modulus among all the eigenvalues of the associated monodromy matrix, and it is further minimized from the previous work (*Case 1*). Therefore, the convergence rate of the biped system is improved by the proposed control strategy as compared with the previous work in [10].

From the optimization results presented earlier in this section, it is straightforward to see that the cost function, i.e., the second largest modulus of all the eigenvalues, is minimized from 0.95 in *Case 1* to 0.57 in *Case 2*. In order to show the improvement in the rate of convergence, the controller design in both cases are simulated and compared. In Fig. 3, the last two steps of the simulations for both cases are compared. Because of the smaller eigenvalues in *Case 2* than in *Case 1*, the trajectories in the right plot reaches the steady state after twelve steps, which illustrates the faster convergence rate of *Case 2* than *Case 1*.

C. Robustness

The improvement in the convergence rate can also affect the robustness of the system. As mentioned, the biped is simulated with some initial tracking errors to see if it will converge back to the desired gait. Also, this kind of initial errors can be caused by an external disturbance such as a push. Therefore, if the biped system has not recovered from a disturbance yet, it might lead to a fall if the system encounters a new disturbance in this situation. In other words, the convergence rate is related to the system's ability to accommodate perturbations from the environment.

Inspired by [7], two sets of simulations corresponding to different external perturbations are simulated to show the high robustness of the proposed method.

1) External force:
   Gradually increasing an external force at a rate of 0.5N per step applied at the center of mass of the robot.
2) Slope of the walking terrain:
   Gradually increasing the slope of the walking terrain at a rate of one degree per step.

In these two simulations, the walking speed is plotted to show the effects of external perturbations on walking. As shown in Fig. 4, the red lines, which correspond to the proposed control design, have a stiffer tendency on the walking speed. The blue lines, which correspond to the prior control design, show that the prior control design is more sensitive to the external perturbations.

V. CONCLUSIONS

In this study, feedback controller design based on input-output linearization is synthesized to achieve orbitally exponential stabilization of underactuated bipedal walking. Similar to the HZD approach, the full-order walking dynamics are established to include a continuous SSP and a discrete DSP. The rigid impact between the swing foot and the ground at a foot landing is modeled as an impulse. Because of underactuation, internal dynamics exist, which, along with the state feedback control design, determine the closed-loop stability. The proposed output function design includes a general class of tracking errors to allow for high design freedom, which is important for finding stable internal dynamics through output function optimization. Finally, the validity of the proposed control strategy is shown through walking simulations. Simulation results also show that the proposed walking strategy greatly improves the closed-loop

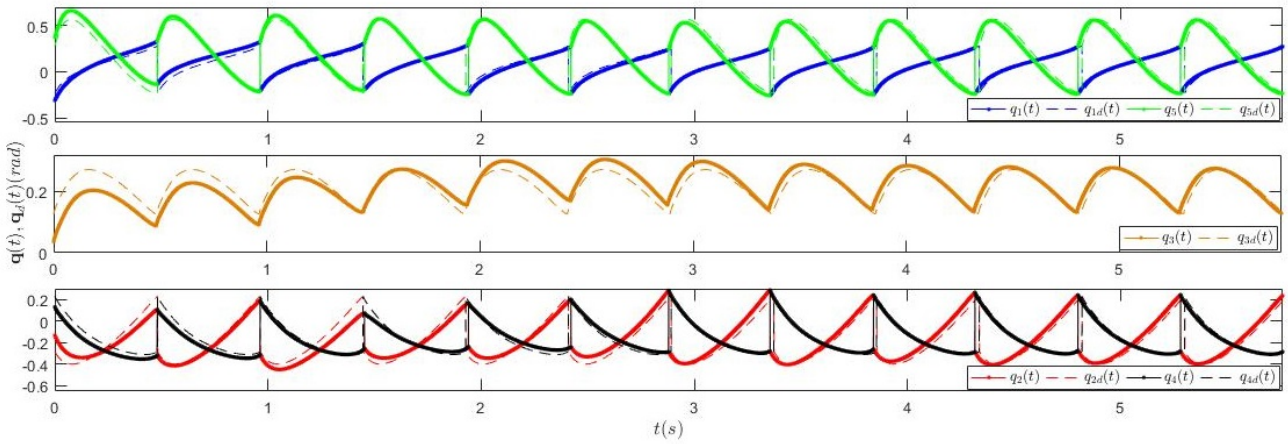

Fig. 2. A twelve-step walking simulation. Control gains: $\mathbf{K}_p = diag([40000, 40000, 40000, 40000])$. Initial conditions: $\mathbf{q}(0^+) - \mathbf{q}_d(0^+) = [-0.08, 0.15, -0.09, -0.1, 0.09]^T$; $\dot{\mathbf{q}}(0^+) - \dot{\mathbf{q}}_d(0^+) = [0.1, -0.15, -0.2, 0.2, 0.2]^T$.

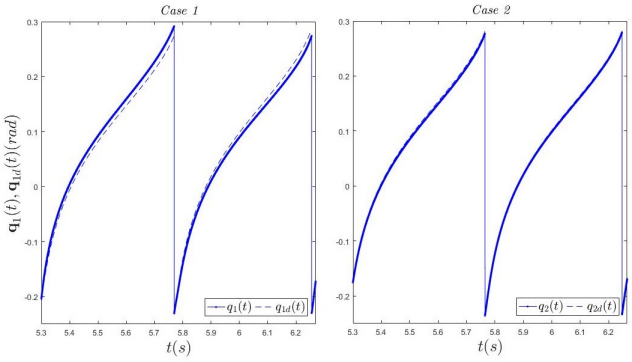

Fig. 3. A tracking performance comparison between *Case 1* (Left) and *Case 2* (Right) during the last two steps of walking simulations.

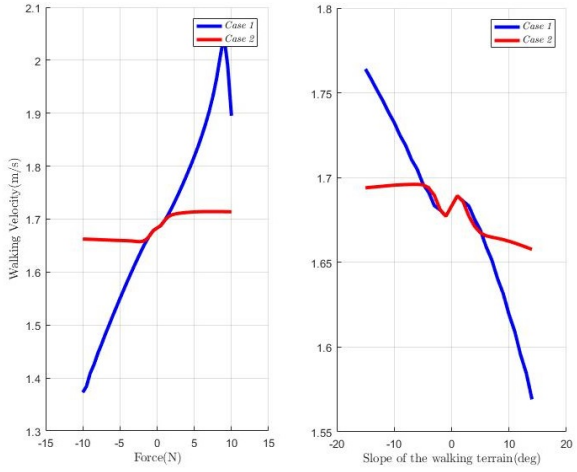

Fig. 4. Robustness improvement of the proposed walking strategy (Case 2) as compared with previous work (Case 1).

convergence rate and robustness as compared with the previous work.

REFERENCES

[1] M. Vukobratovic and B. Borovac, "Zero-Moment Point - Thirty Five Years of its Life," *International Journal of Humanoid Robotics*, vol. 1, no. 1 pp. 157-173, 2004.

[2] S. Kajita, F. Kanehiro, K. Kaneko, K. Fujiwara, K. Harada, K. Yokoi, and H. Hirukawa, "Biped walking pattern generation by using preview control of zero-moment point," in *Proc. of IEEE International Conference on Robotics and Automation*, 2003, pp. 1620-1626.

[3] J. E. Pratt, J. Carff, S. V. Drakunov and A. Goswami, "Capture Point: A Step toward Humanoid Push Recovery," in *Proc. of IEEE-RAS International Conference on Humanoid Robots*, 2006, pp. 200-207.

[4] J. Grizzle, G. Abba, and F. Plestan, "Asymptotically stable walking for biped robots: analysis via systems with impulse effects," *IEEE Transactions on Automatic Control*, vol. 46, no. 1, pp. 51-64, 2001.

[5] E. R. Westervelt, J. W. Grizzle, and D. E. Koditschek, "Hybrid zero dynamics of planar biped walkers," *IEEE Transactions on Automatic Control*, vol. 48, no. 1, pp. 42-56, 2003.

[6] A. D. Ames, E. A. Cousineau, and M. J. Powell, "Dynamically stable bipedal robotic walking with NAO via human-inspired hybrid zero dynamics," in *Proc. of* International Conference on Hybrid Systems: Computation and Control, pp. 135-144, 2012.

[7] B. Griffin and J. Grizzle. "Nonholonomic virtual constraints for dynamic walking," in *Proc. of IEEE Conference on Decision and Control*, pp. 4053-4060, 2015.

[8] T. Yang, E. R. Westervelt, and A. Serrani. "A framework for the control of stable aperiodic walking in underactuated planar bipeds," in *Proc. of IEEE International Conference on Robotics and Automation*, pp. 4661-4666, 2007.

[9] Y. Gu, B. Yao and C. S. G. Lee, "Time-dependent orbital stabilization of underactuated bipedal walking," in *Proc. of American Control Conference.*, pp. 4858-4863, 2017.

[10] Y. Gu, B. Yao and C. S. G. Lee., "Time-dependent Orbital Stabilization of Underactuated Bipedal Walking," in *Automatica* (under review).

[11] M.W. Spong, and M. Vidyasagar, *Robot Dynamics and Control*, New York: Wiley, 1989.

[12] B. Morris and J. W. Grizzle, "Hybrid invariant manifolds in systems with impulse effects with application to periodic locomotion in bipedal robots." *IEEE Transactions on Automatic Control,* vol. 54, no. 8, pp. 1751-1764, 2009.

[13] H. K. Khalil, *Nonlinear Control.* Prentice Hall, 1996.

[14] D. Bainov and P. Simeonov, *Impulsive Differential Equations: Periodic Solutions and Applications.* CRC Press, 1993, vol. 66.